COULD NON-CONDENSIBLE GASES AFFECT HYDROTHERMAL ERUPTIONS ?

R. McKIBBIN

Department of Mathematics, Massey University
Palmerston North, New Zealand

SUMMARY - This paper extends work done previously by the present author (with others) in attempts to construct mathematical models, based on physical conservation laws, which describe the way a hydrothermal eruption progresses. It is assumed that hot fluid which is initially at rest in a porous structure just below the ground surface begins to vent to the atmosphere, beginning at the surface. A "flashing front" progresses downwards through the rock-fluid system, with fluid above moving upwards, driven by pressures which decrease towards atmospheric pressure at the surface. The ground surface is meanwhile eroded away by the lift forces created by the upward-moving fluid which, by the time it gets to the surface, is far less dense than at the flashing front and is moving at high speed. In past work, the fluid was assumed to be pure water (McKibbin, 1989, 1990; Bercich & McKibbin, 1992, 1993). However, as mentioned in McKibbin (1989), the initial motivation for this sequence of studies was to find out what effect the characteristics of a geothermal fluid containing significant amounts of a non-condensible gas such as C02 or H_2S could have on the model of a hydrothermal eruption. In this paper, the presence of non-condensible gases is allowed for in the model; C02 is chosen to represent such components. It is found that large overpressures of non-condensible gases would be needed to significantly affect the erupting fluids potential for lift-driven erosion compared with that of pure water.

1. INTRODUCTION

Possible mechanisms for explaining the transient behaviour of hydrothermal eruptions were outlined in McKibbin (1989, 1990), and extended in Bercich & McKibbin (1992, 1993). The main driving force for expulsion of fluids and solid ground material was hypothesised to be an increased pressure gradient immediately below the surface of the ground due to hot near-surface fluids being suddenly exposed to atmospheric conditions.

In McKibbin (1989, 1990), an attempt was made to formulate the problem, using the principles of conservation of mass, momentum and energy, for both the motion of fluid below ground surface level as well as that of water and rock above ground. The latter part of the problem was set aside, while the first part was dealt with. In fact, it seems that the below-ground motion is the important part from the point of view of attempting to predict how a eruption might begin; the above-ground motion of the expelled material, rising and subsequently falling back onto the eruption surface, is probably more important for inclusion in the prediction of how an eruption slows and ultimately ceases.

In Bercich & McKibbin (1992, 1993), some modifications to the theory and some extensions of the results were made. The simple Darcy's law for a homogeneous liquid-vapour mixture was modified by adding a nonlinear Forchheimer term. The rates of movement of the flashing front and erosion surface were allowed to be different, and the separate speeds were calculated to obtain estimates of the distance each had travelled as the eruption progressed and consequently an estimate of the thickness of the flashing region.

As mentioned in McKibbin (1989), the initial motivation for this sequence of studies was to find out what effect the characteristics of a geothermal fluid containing significant amounts of a non-condensible gas such as C02 or H_2S could have on the potential for, and progress of, a hydrothermal eruption.

In this paper, the presence of non-condensible gases is allowed for in the model; C02 is chosen to represent such components. Appropriate modifications of the governing equations are made.

2. MATHEMATICAL MODEL

2.1 Assumptions

Assumptions in the modelling, which closely follow those used previously, include the following:

- The motion is in the vertical direction only.
- The fluid below the flashing zone is motionless.
- The flowing fluid is a homogeneous mixture of liquid and gas; the ground fluid before decompression is at boiling conditions, but not compressed liquid.
- The process is quasi-steady, i.e. the eruption is in progress, but, because the speed of the fluid towards the surface is large relative to those of the flashing front and erosion surface, the flow is modelled as steady over short periods of time.
- The fluid lifts the rock particles at the surface by overcoming gravitational and cohesion forces.

- Heat transfer between rock and fluid is ignored, and the process is modelled as adiabatic.
- The fluid and gas phases are in thermal equilibrium within the flashing zone.
- Capillary pressure is negligible, so the liquid and total gas pressures are equal.
- The non-condensible gas in the liquid and gas phases are in equilibrium according to Henry's law.

2.2 Preliminary theory

There are two moving boundaries to the flashing zone where underground fluid movement takes place [see Figure 1(a)]. The lower boundary, termed the "flashing front", propagates downward into the stationary fluid in the rock matrix at speed V. The boundary formed by the eroding ground surface above also propagates downward; its speed is V_{er}.

The flashing front moves at speed V into a fluid-filled medium of porosity ϕ where the fluid has temperature T_d, non-condensible gas pressure p_{nd}, liquid saturation $S_{\ell d}$, density ρ_{fd}, and specific enthalpy h_{fd}. Parameters concerned with conditions at the flashing front depth have a 'd' subscript whilst those associated with conditions at the top (eroding) surface, where pressure p is 1.01325 bar absolute (atmospheric pressure), have a 't' subscript. The local average fluid particle velocity is V_f. Subscripts r, n and f denote the rock, non-condensible gas and fluid respectively, while ℓ and g denote the liquid and gas phases. Subscript v denotes water vapour.

The mass fractions of C02 in the liquid and gas phases of the fluid are Y_ℓ and Y_g respectively. The water is assumed to be at saturated (boiling) conditions with the vapour pressure (partial pressure of water gas) at temperature T given by

$$p_v = p_{sat}(T) \qquad (1)$$

The total fluid pressure **p** (equal to both the liquid and the total gas pressures) is given by

$$p = p_\ell = p_g = p_v + p_n \qquad (2)$$

The partial pressure p_n of the CO_2 in the gas phase is related to the mass fraction of C02 dissolved in the liquid phase by Henry's law in the approximate form:

$$p_n = K_H(T)\, Y_\ell \frac{M_{H_2O}}{M_{CO_2}} \qquad (3)$$

where $K_H(T)$ is the Henry's law constant, which is dependent on temperature, and M_{H_2O}, M_{CO_2} are the gram molecular weights (18 and 44 respectively) of water and CO_2.

2.2 Conservation laws

The technique is to set up, and refer all moving quantities relative to, a frame of reference which moves downward at the same speed V as the flashing front [see Figure 1(b)]. Because the motion is assumed to be quasi-steady, the frame of reference can be treated as inertial for the short periods of time considered. Within this frame, the flow is assumed steady.

Conservation of mass

Figure 1(a) shows the flashing front moving downwards at speed V into a motionless fluid in the pores of the medium of uniform porosity ϕ. If, relative to a frame of axes moving with the flashing front [Figure 1(b)], the fluid volume flowrate per unit area (specific discharge) is w_f, then the separate liquid and gas phase mass flowrates for water and C02 per unit area through this region and the flashing zone are respectively

$$m_\ell^w = (1 - Y_\ell) S_\ell \rho_\ell w_f$$

$$m_g^w = (1 - Y_g)(1 - S_\ell) \rho_g w_f$$

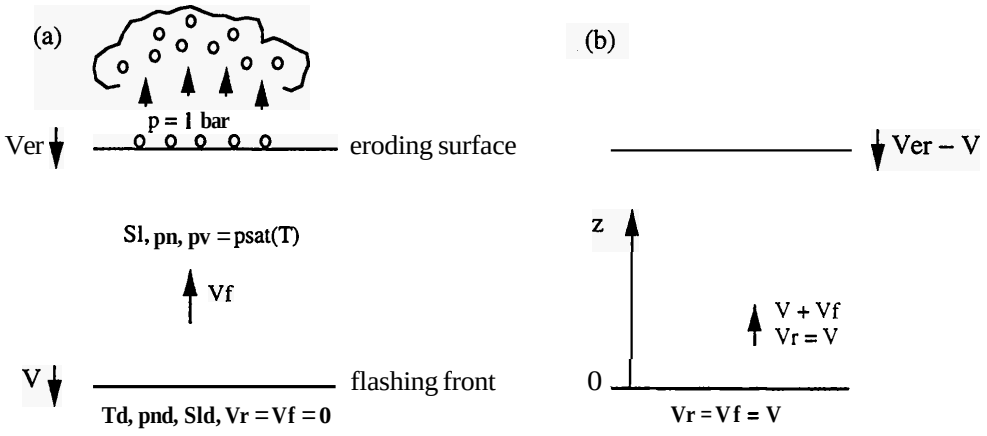

Figure 1: Schematic of flows: (a) relative to fixed axes; (b) relative to frame of reference moving downwards at speed V with the flashing front.

and

$$m_\ell^n = Y_\ell S_\ell \rho_\ell w_f$$

$$m_g^n = Y_g(1 - S_\ell)\rho_g w_f$$

Here, S_ℓ is the liquid saturation (volume fraction of liquid in the two-phase fluid) and ρ_ℓ and ρ_g are the densities of the liquid and gas phases of the fluid. Conservation of the two components implies that the separate total (liquid + gas) mass flowrates for water and non-condensible gas are constant:

$$m_w = m_\ell^w + m_g^w = \rho_w w_f$$

and

$$m_n = m_\ell^n + m_g^n = \rho_n w_f$$

where the separate overall water and non-condensible gas densities in the mixture are

$$\rho_w = (1 - Y_\ell)S_\ell \rho_\ell + (1 - Y_g)(1 - S_\ell)\rho_g$$

and

$$\rho_n = Y_\ell S_\ell \rho_\ell + Y_g(1 - S_\ell)\rho_g$$

Conservation of mass implies that

$$m_w = m_{wd} = \rho_{wd} w_{fd} = \rho_{wd}\phi V$$

and

$$m_n = m_{nd} = \rho_{nd} w_{fd} = \rho_{nd}\phi V$$

where

$$\rho_{wd} = (1 - Y_{\ell d})S_{\ell d}\,\rho_{\ell d} + (1 - Y_{gd})(1 - S_{\ell d})\rho_{gd} \quad (4)$$

and

$$\rho_{nd} = Y_{\ell d}S_{\ell d}\,\rho_{\ell d} + Y_{gd}(1 - S_{\ell d})\rho_{gd} \quad (5)$$

are the respective densities at the flashing front.

The total fluid mass flowrate, relative to the moving frame of axes [Figure 1(b)], is constant, and is given by

$$m_f = m_w + m_n = \phi\rho_f(V + V_f) \quad (6)$$

where V_f is the interstitial fluid speed. At the "flashing front", $V_f = 0$ and hence

$$m_f = \phi\rho_f(V + V_f) = \phi\rho_{fd}V \quad (7)$$

The fluid mixture densities ρ_f, ρ_{fd} are

$$\rho_f = S_\ell\rho_\ell + (1 - S_\ell)\rho_g = \rho_w + \rho_n$$

$$\rho_{fd} = S_{\ell d}\rho_{\ell d} + (1 - S_{\ell d})\rho_{gd} = \rho_{wd} + \rho_{nd}$$

The rock has zero absolute velocity. Relative to the moving frame, the rock mass flowrate m_r is constant and is given by

$$m_r = (1 - \phi)\rho_r V$$

Conservation of momentum

The fluid volume flowrate per unit area w_f relative to the moving frame of axes is given by the simple Darcy's Law:

$$w_f = \frac{k}{\mu_f}\left(-\frac{dp}{dz} - \rho_f g\right) + \phi V \quad (8)$$

where the term ϕV is associated with the moving reference frame. Bercich & McKibbin (1992, 1993) deduced that a nonlinear extension to this equation, through addition of the so-called Forchheimer term [proportional to $(\phi V_f)^2$ in this case] was important only for large permeabilities. The linear Equation (8) will be used in this study. For the boiling mixture, the dynamic viscosity is taken to be

$$\mu_f = \mu_\ell S_\ell \mu_g(1 - S_\ell)$$

With the assumption that the boiling fluid is moving as a homogeneous two-phase mixture, the separate liquid and vapour mass flowrates per unit area are

$$m_\ell = S_\ell\rho_\ell w_f \quad \text{and} \quad m_g = (1 - S_\ell)\rho_g w_f$$

and the total mass flow per unit area is

$$m_f = m_\ell + m_g = \rho_f w_f$$

Substitution into Equation (6), rearrangement and use of Equations (7) and (8) gives

$$V_f = \left(\frac{\rho_{fd}}{\rho_f} - 1\right)V = \frac{k}{\phi\mu_f}\left(-\frac{dp}{dz} - \rho_f g\right) \quad (9)$$

From Equation (7) it can also be deduced, by applying the surface boundary conditions, that

$$V = \frac{V_{ft}}{\frac{\rho_{fd}}{\rho_{ft}} - 1} = \frac{V_{ft}}{\frac{v_{ft}}{v_{fd}} - 1} \quad (10)$$

where v is the specific volume. This equation relates the flashing front speed to the speed and density of the fluid as it reaches the surface. The overall volume expansion factor for the flashing fluid as it rises from the bottom to the surface is given by

$$v_{rat} = \frac{v_{ft}}{v_{fd}} = \frac{\rho_{fd}}{\rho_{ft}} \quad (11)$$

Conservation of energy

The vertical energy flowrate per unit area is

$$q_e = m_\ell h_\ell + m_g h_g = m_f h_f$$

where

$$h_f = \frac{\rho_g h_g + S_\ell(\rho_\ell h_\ell - \rho_g h_g)}{S_\ell\rho_\ell + (1 - S_\ell)\rho_g} \quad (12)$$

is the flowing enthalpy of the fluid.

Boundary conditions at the flashing front give

$$q_e = m_f h_{fd}$$

Because q_e is conserved and m_f is constant, $h_f = h_{fd}$ and the fluid flow is isenthalpic.

Mixture specific enthalpies are calculated using

$$h_\ell = (1 - Y_\ell)h_{w\ell} + Y_\ell(h_{ng} + h_{sol}) \quad (13)$$

$$h_g = (1 - Y_g)h_v + Y_g h_{ng} \quad (14)$$

Rearrangement of Equation (12) gives the liquid saturation in terms of the flowing enthalpy:

$$S_\ell = \frac{\rho_g (h_g - h_f)}{(\rho_\ell - \rho_g) h_f - (\rho_\ell h_\ell - \rho_g h_g)} \quad (15)$$

and the enthalpy at the flashing front is given in terms of fluid parameters there by

$$h_{fd} = \frac{\rho_{gd} h_{gd} + S_{\ell d} (\rho_{\ell d} h_{\ell d} - \rho_{gd} h_{gd})}{\rho_{fd}} \quad (16)$$

Equation **(9)** can be rearranged to give an expression for the pressure gradient at any point in the flow:

$$\frac{dp}{dz} = -\rho_f g - \frac{\mu_f \phi V}{k}\left(\frac{\rho_{fd}}{\rho_f} - 1\right) \quad (17)$$

3. EXPANSION CALCULATIONS

During flow from the flashing front to the erosion surface, the fluid mixture enthalpy h_f and the overall mass fraction of the non-condensible gas Y are both conserved.

First, in order to find how the presence of CO_2 affects conditions at the discharge into the atmosphere, the change in fluid condition from the bottom of the flow to the top was calculated for various bottom values of temperature T_d, partial CO_2 pressures p_{nd} and liquid saturation values $S_{\ell d}$.

The calculation procedure was as follows:

1. Use Equation (1) to find $p_{vd} = p_{sat}(T_d)$.

2. Use Equation (2) to find the total pressure:

$$p_d = p_{\ell d} = p_{gd} = p_{vd} + p_{nd}$$

3. Calculate the separate densities of water and CO_2 at prevailing bottom conditions, and thereby the mass fraction of non-condensible gas Y_{gd} in the gas phase from

$$Y_{gd} = \frac{\rho_{ngd}}{\rho_{vd} + \rho_{ngd}}$$

4. Use Henry's law [Equation (3)] to calculate the mass fraction $Y_{\ell d}$ of non-condensible gas dissolved in the liquid phase.

5. Calculate the overall mass fraction Y of non-condensible gas using Equations (4) and (5) and

$$Y = Y_d = \frac{\rho_{nd}}{\rho_{wd} + \rho_{nd}}$$

6. Calculate the specific enthalpies of the components and thereby the the overall fluid mixture enthalpy h_{fd} using Equations (13), (14) and substitution into (16).

The thermodynamic properties of the two components were calculated from well-known correlations.

Having established the conserved values **Y** ($=Y_d$) and h ($=h_{fd}$), the focus moved to atmospheric pressure at the erosion surface, where $p_t = 1.01325$ bars absolute. Both the temperature T_t and liquid saturation $S_{\ell t}$ were found so that the corresponding Y_t and h_{ft} values were the same as those at the bottom.

One of the important indicators is the expansion parameter v_{rat}, given by Equation (11), which is the ratio between the specific volume of the fluid as it vents to atmosphere to that at the flashing front. Figure 2 shows values for the case of pure water (Y = 0) where v_{rat} is plotted against T_d for each value of $S_{\ell d}$ in the range 0.0 (0.1) 1.0. The main question asked here is: what is the effect on this parameter of increasing values of Y?

A variety of results are presented in Figure 3. Each shows: (a) the overall non-condensible gas fraction Y; surface values of (b) temperature T_t; (c) liquid saturation $S_{\ell t}$; (d) non-condensible gas partial pressure p_{nt}; and (e) volume ratio v_{rat} [Equation (11)], for $S_{\ell d} = 0.1$ and 1.0, and each for $p_{nd} = 0$, 10, 25 and 50 bars. All are shown as functions of flashing front temperature T_d for various values of partial pressure p_{nd} of CO_2.

All of the above parameters depend only on the thermodynamic assumption that the fluid emerges at atmospheric pressure. Further assumptions about the force needed to eject solid material at the erosion surface leads to values for V_{ft} and thence to flashing front speed V from Equation (10). Some typical calculated values of V are shown in Figure 4.

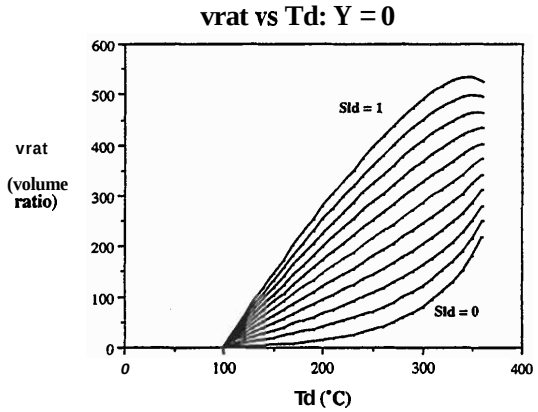

Figure 2: Values of the specific volume ratio $v_{rat} = v_{ft}/v_{fd}$ for transition from the reservoir state to atmospheric pressure [for cases $S_{\ell d} = 0$ (0.1) 13.

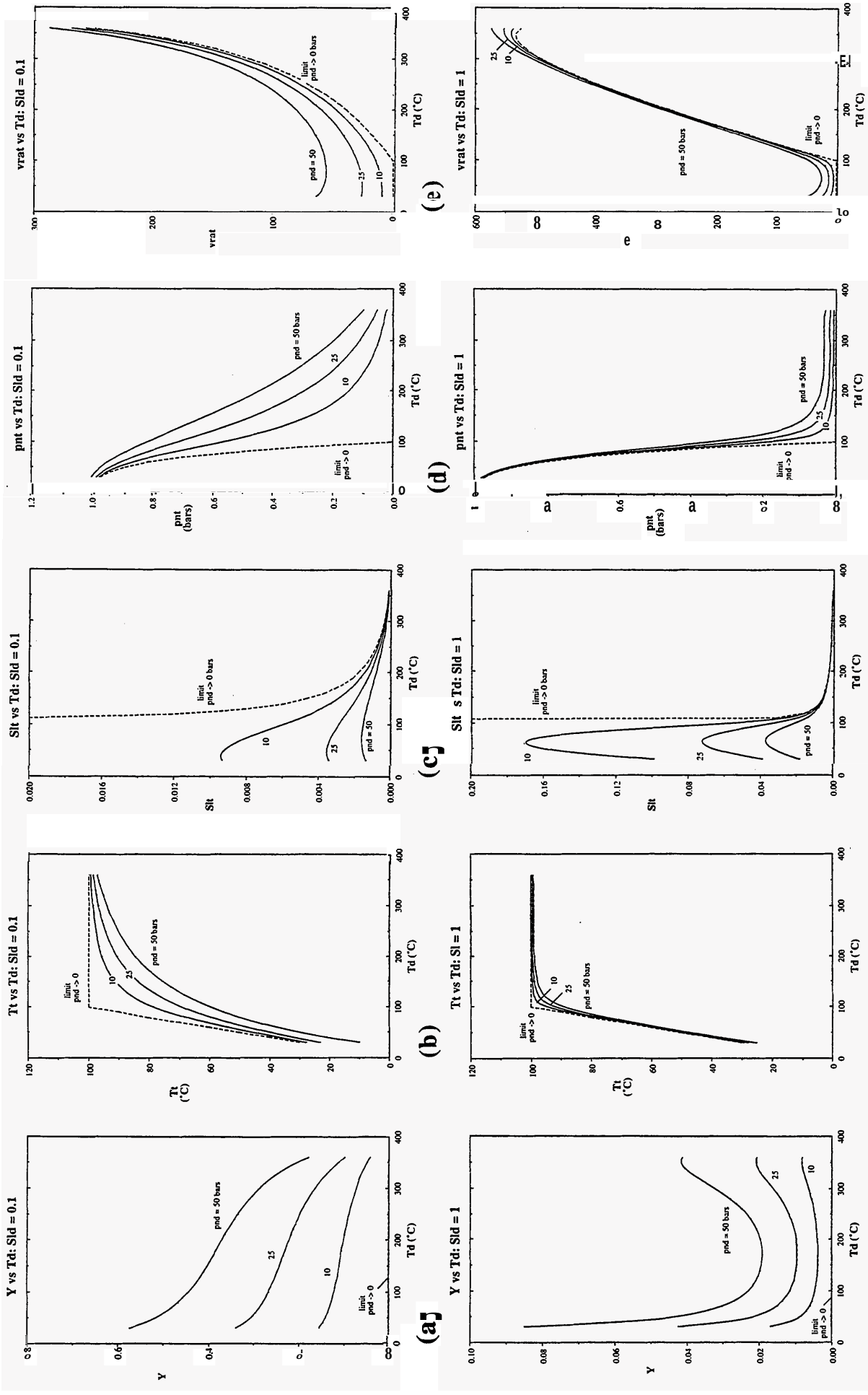

Figure 3: (a) The overall non-condensible gas fraction Y; surface values of (b) temperature T_t; (c) liquid saturation $S_{\ell t}$; (d) non-condensible gas partial pressure p_{nt}; and (e) volume ratio v_{rat}, all as functions of flashing front temperature T_d for flashing front CO_2 partial pressures p_{nd} = 0, 10, 25 and 50 bars. In each case, the upper graphs are for $S_{\ell d}$ = 0.1, and the lower ones are for $S_{\ell d}$ = 1.0. See the text for explanation and discussion.

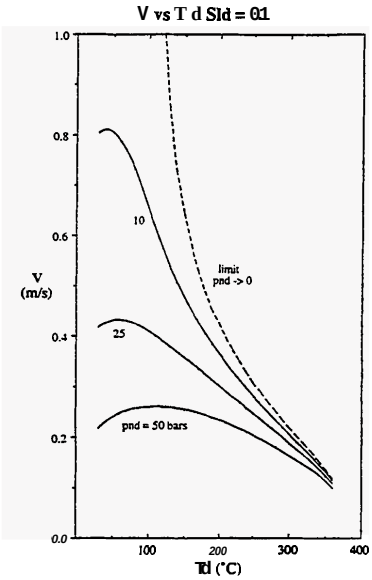

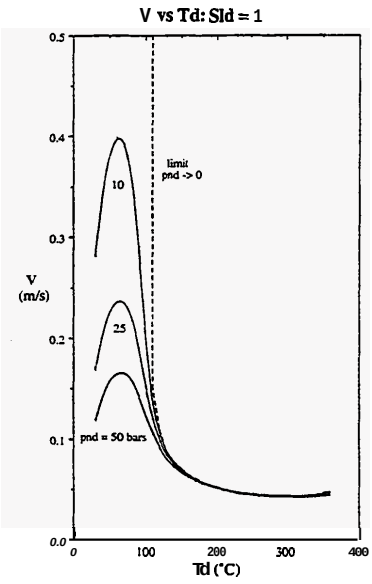

Figure 4: Typical flashing front speed V as a function of flashing front temperature T_d for CO_2 partial pressures p_{nd} = 0, 10, 25, 50 bars. See text for discussion.

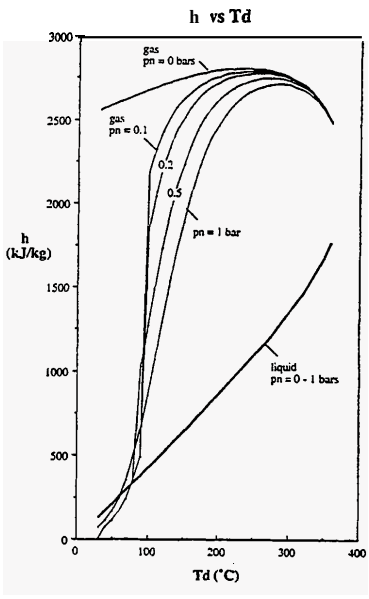

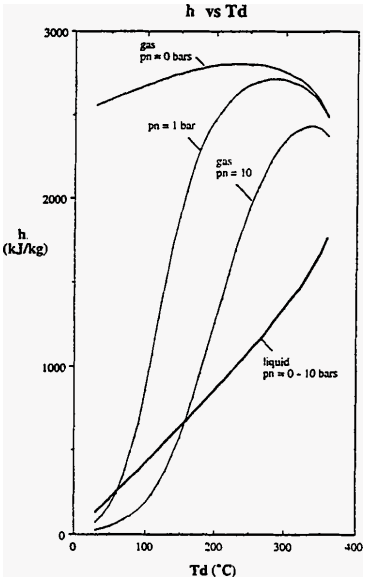

Figure 5: Variation of the separate liquid and gas phase specific enthalpies h_ℓ and h_g with temperature T and CO_2 partial pressure p_n.

For any total pressure p between p_d and p_t, the condition of the fluid can be calculated under the assumption that locally the system is in thermodynamic equilibrium. Application of Equation (17) allows calculation of the the relationship between pressure profile and the distance the fluid has travelled, and thereby an estimate of the thickness of the flashing zone. The method and examples are shown in Bercich & McKibbin (1992, 1993). In this paper, however, attention is focussed on the results given in Figures 2 and 3.

4. RESULTS and DISCUSSION

4.1 Fluid properties

Figure 2 shows the ratio between the specific volume of pure water as it emerges at atmospheric pressure at the erosion surface and that *in situ* at the flashing front, for T_d between 100 and 370 °C, and for $S_{\ell d}$ = 0 (0.1) 1. As discussed in McKibbin (1990), it is this expansion which gives rise to the high velocities and consequent erosion potential of the escaping fluid. The greatest potential is for liquid reservoir conditions; the presence of a steam phase reduces the possible effect, with a dry system having least capability for expansion as the pressure drops to atmospheric conditions. This in itself may give a clue to the effect of the presence of a non-condensible gas component.

Figure 3(a) shows how the overall mass fraction of CO_2 in the reservoir fluid depends on its partial pressure for the two cases where $S_{\ell d}$ = 0.1 (gas phase occupies 90 % of the pore volume at depth) and $S_{\ell d}$ = 1 (liquid phase only in porous matrix). In the first case, the overall mass fraction Y is close to that of the mass fraction Y_g of CO_2 in the gas phase. In the second case, all of the non-condensible gas is dissolved in the liquid and even very high CO_2 overpressures produce relatively small Y values. Note that it is possible for T_d to be less than 100 °C provided the total gas pressure in the reservoir is larger than atmospheric pressure.

The temperature T_t of the emerging fluid is shown in Figure 3(b) for the same parameters as mentioned above. The total pressure of the escaping fluid is atmospheric pressure, while the water contributes only the vapour pressure $p_{sat}(T_t)$. A large non-condensible gas component in the gas phase will therefore reduce the surface temperature significantly compared with pure water - this is demonstrated in the upper graph where $S_{\ell d}$ = 0.1, and may be compared with the lower graph for $S_{\ell d}$ = 1, where some of the CO_2 remains dissolved in the escaping fluid and produces only a small reduction from that corresponding to pure water. The dashed line, for Y = 0, represents an escape temperature of 100 °C for any cases where T_d > 100 °C, while for T_d < 100 °C, the line is a limiting envelope which is approached as the pressure p_d at the flashing front approaches

atmospheric pressure. (Note that, for p_d below atmospheric pressure, there will be no ejective force.)

The effect of the presence of non-condensible gas in the reservoir fluid on the liquid saturation $S_{\ell t}$ of the fluid as it emerges is shown in Figure 3(c). The dissolved non-condensible gas moves into the gas phase as the total pressure decreases (with accompanying decrease in C02 partial pressure) as the fluid moves upwards. **As** might be anticipated, an increase in C02 content within the reservoir increases the dryness of the escaping fluid. The effect seems to be relatively more marked in a drier system ($S_{\ell d} = 0.1$) than in the liquid case. In the latter case ($S_{\ell d} = 1$), the effects are greatest for T_d near 100 "C.

Figure 3(d) begins to illustrate the large density decreases (and specific volume increases) that occur as the fluid moves upwards. Very large *in situ* partial pressures p_{nd} of non-condensible gas are reduced to relatively very small p_{nt} values at the erosion surface, with the reductions being greater for higher temperatures. For liquid reservoir conditions, C02 partial pressures at the surface are very small; this is due to the relatively smaller amount of non-condensible gas in the fluid mixture [see Figure 3(a)].

As mentioned in 33 above, the volume ratio v_{rat} is an important indicator of potential for erosion. Values of v_{rat} for pure water were given in Figure **2.** Now Figure 3(e) shows how two of the curves in Figure **2,** namely those for $S_{\ell d} = 0.1$ and $S_{\ell d} = 1$, are modified by the presence of a non-condensible gas. While the effect seems more marked in the first case (upper graph), the actual values of v_{rat} there are much smaller than those for pure water in the liquid reservoir case (lower graph). The latter case shows little effect for $T_d > 150$ °C; the greatest effect is for T_d near 100 °C, and then only for large C02 overpressures. The erosion potential, for systems where the non-condensible gas pressure is no larger than the water vapour pressure, depends much more strongly on the *in situ* temperature T_d than on the C02 partial pressure p_{nd}.

The values shown in the above graphs for $T_d < 100$ "C are probably not applicable to geothermal systems, but may be useful parameters for consideration when C02 or other non-condensible gas underground reservoir storage facilities are being proposed (see Weir *et af.,* 1996a, 1996b, for example).

4.2 Flashing front speed

Figure 4 shows some typical results for the speed V of the flashing front. **As** mentioned in 33 above, the calculated values depend on some assumptions about the material being ejected at the erosion surface and some geometrical properties of the porous matrix. Results presented in Figure 4 therefore provide an opportunity to make only qualitative deductions about the effects of a non-condensible gas. **As** can be seen, the general effect is to reduce the speed compared to that in the pure water case, with the effect being far greater for a system with a small liquid saturation ($S_{\ell d} = 0.1$); at higher temperatures, the effect is reduced. The effects for the liquid system are very small for T > 100 "C.

4.3 Energy content

In the adiabatic model explored here, the fluid flow is isenthalpic. It seemed appropriate to investigate in more detail the effect of non-condensible gas content on the specific enthalpies (and thereby the energy content) of the *in situ* liquid and gas phases. In the calculations performed above, the total energy content of the fluid mixture at the flashing front was determined by taking an appropriate linear combination of the separate values.

Figure 5 shows how the separate liquid and gas phase specific enthalpies h_ℓ and h_g vary with temperature T and C02 partial pressure p_n. The left-hand graph shows examples where $0 \le p_n \le 1$ bar abs., while the other shows the effect for p_n up to 10 bars abs.

A notable observation is that the specific enthalpy of the liquid phase changes very little with C02 content. This is due to the small mass fraction of non-condensible gas dissolved in the water even at high partial pressures. The main effect is in the gas values. For $p_n = 0$ bars, the pure water values are obtained. In general, increasing p_n leads to decreasing values of h_g. The apparent cutoffs for low p_n values in the left-hand graph are due to the requirement that the total gas pressure be greater than atmospheric pressure for eruptions to take place (for the case $S_{\ell d} = 0.8$). The right-hand graph demonstrates how the specific enthalpy of the water vapour is significantly degraded by the presence of a low-enthalpy gas-phase component.

6. SUMMARY and CONCLUSIONS

The picture is rather complicated. While all calculations were made for a range of reservoir temperatures T_d, another way to compare might have been to calculate for ranges of reservoir total pressures p_d. The current results should be therefore be viewed as consideration of how injections or buildups of non-condensible gases in otherwise fixed-temperature systems affects the potential for hydrothermal eruptions.

One general conclusion is that non-condensible gases have greater effect on the fluid properties in regions where the liquid saturation is low, i.e. where the gas phase is the dominant volume fraction. However, the speed of the flashing process is also slowed down the most in such regions, and the specific enthalpy is significantly reduced.

Since the solubility, in terms of mass, of C02 in liquid water is small, such effects are less in liquid systems. However, because liquid water has the greatest expansion potential in any case (see Figure **2),** it seems that the most important parameter ranges for eruption potential are high temperature and high liquid saturation.

Based on the results found in this work, no definite statement can be made as to whether or not the presence of moderate amounts of non-condensible gases in a water system enhance the chance of hydrothermal eruptions. Further work integrating the fluid properties with eruption progress calculations may clarify the matter.

REFERENCES

Bercich, B.J. and McKibbin, R. (1992). Modelling the development of natural hydrothermal eruptions. *Proceedings of the 14th New Zealand Geothermal Workshop 1992*, University of Auckland, 305-312. Corrigendum (1993) *Proceedings of the 15th New Zealand Geothermal Workshop 1993*, University of Auckland, 345-346.

McKibbin, R. (1989). An attempt at modelling hydrothermal eruptions. *Proceedings of the 11th New Zealand Geothermal Workshop 1989*, University of Auckland, 267-273.

McKibbin, R. (1990). Mathematical modelling of hydrothermal eruptions. 1990 International Symposium on Geothermal Energy, *Geothermul Resources Council Transactions*, v. 14, 1309-1316.

McKibbin, R. and McNabb, A. (1996) Deep hydrothermal systems: Mathematical modelling of hot dense brines containing non-condensible gases. *Proceedings of the International Conference on Porous Media and Their Applications in Science, Engineering and Industry, June 1996*, Engineering Foundation & Institute of Industrial Mathematical Sciences, 264-283.

Weir, G.J., White, S.P. and Kissling, W.M. (1996a) Reservoir storage and containment of greenhouse gases. *Transport in Porous Media*, v. 23 (1), 37-60.

Weir, G.J., White, S.P. and Kissling, W.M. (1996b) Reservoir storage and containment of greenhouse gases, 11: Vapour-entry pressures. *Transport in Porous Media*, v. 23 (1), 61-82.